Distribution of Si and Al in Clintonites: A Combined NMR and Monte Carlo Study

J. Sanz,*,† C. P. Herrero,† and J.-L. Robert‡

Instituto de Ciencia de Materiales, C.S.I.C. Cantoblanco, 28049 Madrid, Spain, and Institut des Sciences de la Terre, UMR 6113, CNRS-Université d'Orléans, 45071 Orléans Cedex 2, France

Received: January 24, 2003; In Final Form: June 2, 2003

The distribution of silicon and aluminum atoms over the tetrahedral sheets of clintonites (aluminum-rich phyllosilicates 2:1) has been studied by ^{29}Si and ^{27}Al magic-angle-spinning NMR spectroscopies. According to the ^{29}Si NMR spectra, no silicon atoms are present in adjacent tetrahedra; however, several environments have been detected in the ^{27}Al NMR signal, proving that these aluminosilicates do not adhere to Loewenstein's rule. The atom distribution has been simulated by a Monte Carlo procedure. From the results of these simulations, a further dispersion of silicon atoms over the tetrahedral sheets has been found, indicating a homogeneous dispersion of the electrostatic charge over the phyllosilicate layers. In contrast, a maximum dispersion of charges must be discarded in the layers of studied clintonites. Finally, an analysis of structural factors controlling this kind of cation distribution is given.

Introduction

Clintonite is a trioctahedral brittle mica (phyllosilicate 2:1) with an ideal composition of $Ca(SiAl_3)(Mg_2Al)O_{10}(OH)_2$, i.e., with a fraction of tetrahedral aluminum x_{Al} of 0.75.[1] Previous X-ray diffraction studies of clintonites showed that the crystal symmetry was monoclinic, *C*2/*m* space group, and that tetrahedral and octahedral cation distributions were disordered in the long range.[2−4] The short-range distribution of Si and Al atoms on the tetrahedral networks of aluminosilicates has been studied over the past decades with solid-state nuclear magnetic resonance (NMR) methods.[5−9] In aluminosilicates with more tetrahedral Si loading than Al loading, it is well established that adjacent tetrahedra do not simultaneously contain aluminum (the so-called Loewentein's rule),[10] in both natural and synthetic materials. However, this rule has to be necessarily violated for materials containing more aluminum than silicon in the tetrehedral sheets that, although rare, can be found in nature, as in the case of the phyllosilicate clintonite. Violation of Loewenstein's rule has been also reported in aluminosilicates far from thermodynamic equilibrium.[8,9]

Computer modeling of the cation distribution is a complementary method for obtaining insight into Si and Al ordering. Along this line, Monte Carlo simulations have been employed earlier to derive cation distributions compatible with the local cation ordering deduced from ^{29}Si NMR spectroscopy. This kind of simulation allowed us to determine the main characteristics of the distribution of Si and Al on two-dimensional tetrahedral networks of phyllosilicates,[11−13] as well as on the three-dimensional frameworks of tectosilicates.[14−17] To explain the experimental NMR results, short-range effective interactions between tetrahedral cations were derived. In fact, interactions between nearest and next-nearest cations have been found to be sufficient to explain NMR spectra of these minerals.[11,14] Other theoretical methods, such as the so-called "cluster variation method", have also provided insight into cation distribution in micas.[12,18]

In this paper, we study the distribution of Si and Al in good-quality synthetic clintonite samples with several compositions by ^{29}Si and ^{27}Al NMR spectroscopy. Our results indicate that a silicon−silicon avoidance is fulfilled, and that an effective repulsion between silicon atoms is present beyond nearest-neighbor tetrahedra. A Monte Carlo method has been employed to determine cation distributions compatible with the observed relative intensities of the NMR lines in the ^{27}Al NMR spectra. A discussion of structural reasons that favor the observed distributions of Si and Al is given in the last part of the paper.

Methods

Sample Preparation. Trioctahedral phyllosilicates of the series $Ca^{2+}(Si_{1+z}Al_{3-z})Mg_{2+z}Al_{1-z}O_{10}OH_2$ have been synthesized with z in the range of 0−0.33. The index z is related to the Al and Si fractional contents of the tetrahedral sheet, x_{Al} and x_{Si}, respectively, by the expressions $x_{Al} = (3 - z)/4$ and $x_{Si} = (1 + z)/4$. Samples were prepared by hydrothermal synthesis at 600 °C and 1 kbar, using run durations of 2 months. The starting products were gel mixtures with the appropriate compositions, obtained according to the gelling method described by Hamilton and Henderson.[19] The gel mixtures were introduced in a gold tube sealed by arc welding, accompanied with the appropriate amount of distilled water. After the synthesis in Tuttle-type cold-sealed externally heated pressure vessels, the samples were quenched and examined by optical and X-ray diffraction (XRD) methods to confirm the single-phase character. Unit cell parameters of clintonites were determined with an INEL CPS120 diffractometer equipped with a position sensitive curved detector, using Si as an external standard. Calibration was achieved according to the procedure described by Roux and Volfinger.[20]

Chemical analysis carried out with the inductively coupled plasma (ICP) technique showed deviations from expected values of <1% for all elements. Prepared samples displaying x_{Si} values ranging from 0.25 to 0.33 cover the compositional range found in nature for clintonite samples. The resulting tetrahedral compositions, calculated on the basis of 10 oxygens and two hydroxyl groups per structural formula, are given in Table 1.

† C.S.I.C. Cantoblanco.
‡ CNRS-Université d'Orléans.
* Corresponding author.

10.1021/jp030097m CCC: $25.00
Published on Web 07/29/2003

TABLE 1: Unit Cell Parameters Deduced from XRD Patterns of Clintonites

	a (Å)	*b* (Å)	*c* (Å)	β (deg)
Si_1Al_3	5.210(1)	9.001(1)	9.803(1)	100.22(1)
$Si_{1.12}Al_{2.88}$	5.207(1)	9.003(1)	9.809(2)	100.23(1)
$Si_{1.25}Al_{2.75}$	5.209(1)	9.006(1)	9.809(2)	100.10(1)
$Si_{1.33}Al_{2.67}$	5.210(1)	9.021(1)	9.819(2)	100.20(1)

Unit cell parameters deduced from XRD patterns are also included in Table 1.

Nuclear Magnetic Resonance. ^{29}Si ($I = {}^1/_2$) and ^{27}Al MAS NMR ($I = {}^5/_2$) spectra were recorded at 79.49 and 104.26 MHz, respectively, with a Bruker MSL-400 spectrometer. The external magnetic field was 9.4 T. All measurements were carried out at room temperature, and samples were spun around the magic angle (54° 44′ with respect to the magnetic field) at 4 and 12 kHz. ^{29}Si and ^{27}Al NMR spectra were recorded after $\pi/2$ and $\pi/8$ pulse excitations, respectively (4 and 2 μs, respectively), and intervals between successive accumulations (6 and 2 s, respectively) were chosen in an effort to avoid saturation effects. TMS and $AlCl_3$ solutions were used as external standard references. Errors in band positions are less than 0.5 ppm. To preserve the quantitative analysis, no mathematical procedures of NMR signal treatment, such as multiplication by an exponential function, were used. The fitting of MAS NMR spectra was carried out with the Bruker WINFIT program.[21] This program allows the position, line width, and intensity of NMR components to be determined by using a nonlinear iterative least-squares method. However, quadrupole constants C_Q and η must be determined by a trial and error procedure. For quantitative purposes, the addition of spinning sidebands of different components was calculated. Errors in determination of relative band intensities are less than 5%.

Two-dimensional MAS NMR (triple-quantum, single-quantum) experiments were carried out in a 400AV-WB spectrometer by using the MQZQF technique.[22,23] Samples were spun around the magic angle at 15 kHz. 3Q MAS spectra were acquired with a two-pulse sequence, with pulse lengths of 3.6 and 1.5 μs, in which the separation between pulses, 3 μs, was set to approximate the inverse of the quadrupole splitting. After excitation of the triple-quantum coherence, this was transferred into a single-quantum coherence. Finally, the NMR signal was detected after a selective $\pi/2$ pulse of 12 μs. The separation between second and third pulses was set near the rotor period (70 μs). With this technique, second-order quadrupolar broadenings can be attenuated and spectral resolution considerably enhanced, favoring the analysis of ^{27}Al MAS NMR patterns in the isotropic dimension.

Monte Carlo Simulation. The sites occupied by silicon and aluminum cations in the tetrahedral sheets of phyllosilicates form a two-dimensional hexagonal (honeycomb) network. We have carried out Monte Carlo (MC) simulations of the distribution of Si and Al over such a network for different layer compositions, with x_{Si} ranging from 0.25 to 0.33. The simulation cell included 10 000 tetrahedral sites, and periodic boundary conditions were assumed. Cation configurations were selected according to the Metropolis procedure.[24] The absence of silicon cations in nearest tetrahedra, derived from ^{29}Si NMR spectra (see below), is included in the simulation by introducing a silicon−silicon effective interaction energy E_1 several times larger than the thermal factor k_BT (in fact, an E_1 equal to $5k_BT$ is enough to have a negligible number of pairs of silicons in adjacent tetrahedra). Here, T is considered the temperature of phyllosilicate formation. To take into account interactions between cations at larger distances, we have considered an effective interaction energy E_2 between silicon atoms in second-nearest tetrahedral sites. For each composition that was studied, we carried out several simulations, changing the effective interaction between cations in second-nearest tetrahedra. Such an effective interaction can be understood as a result of electrostatic interaction between cations with different charges. In fact, E_2 is the so-called atomic interchange energy given by

$$E_2 = 2V_{Si,Al} - V_{Si,Si} - V_{Al,Al}$$

where, for example, $V_{Si,Al}$ indicates the energy of the interaction between Si and Al in next-nearest tetrahedra. This procedure was found earlier to be adequate for describing atomic distributions in silicon-rich phyllosilicates.[11,12] More details on this kind of MC simulations for phyllo- and tectosilicates can be found elsewhere.[11,14]

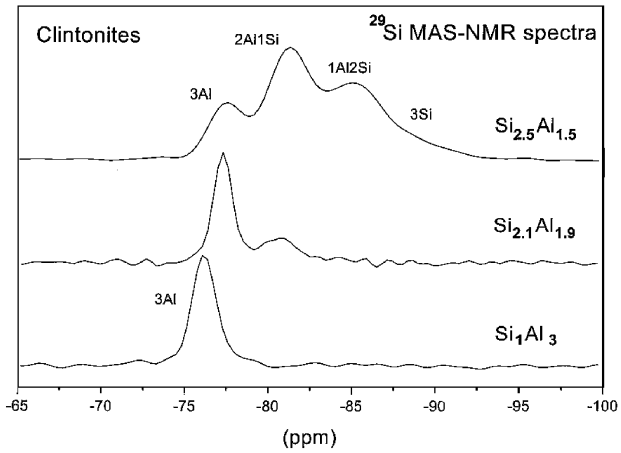

Figure 1. ^{29}Si MAS NMR spectra of clintonite (Si_1Al_3), preiswerkite ($Si_{2.1}Al_{1.9}$), and eastonite ($Si_{2.5}Al_{1.5}$) micas.

Results and Discussion

In clintonites, with the $Ca(Si_{1+z}Al_{3-z})(Mg_{2+z}Al_{1-z})O_{10}OH_2$ composition, the amount of Ca^{2+} is nearly constant as the index z changes, and substitution of Si for Al beyond the $SiAl_3$ composition is offset by replacing Al^{3+} with Mg^{2+} in the octahedral sheet. This fact shows that the negative layer charge is accumulated in the tetrahedral sheets at the expense of that of the octahedral one.

In Figure 1, we present the ^{29}Si MAS NMR spectrum of the synthetic clintonite $Ca(Si_1Al_3)(Mg_2Al)O_{10}OH_2$ ($x_{Si} = 0.25$), along with those of the mica-type materials preiswerkite $Na(Si_{2.1}Al_{1.9})(Mg_{2.1}Al_{0.9})O_{10}OH_2$ ($x_{Si} \sim 0.52$) and eastonite $Na(Si_{2.5}Al_{1.5})(Mg_{2.5}Al_{0.5})O_{10}OH_2$ ($x_{Si} = 0.63$). For clintonites, with compositions approximating $SiAl_3$, one finds in the NMR spectrum a single line, at a chemical shift of approximately −76 ppm. This line displays characteristics similar to that obtained in the case of preiswerkite (at −77.1 ppm), which was ascribed to silicon atoms surrounded by three Al tetrahedra. In the case of eastonite, with a larger amount of Si ($Si_{2.5}Al_{1.5}$ composition), one finds different lines at −77.3, −81, −85, and −89 ppm in the ^{29}Si NMR spectrum, corresponding to Si environments with 3Al, 2Al1Si, 1Al2Si, and 3Si, respectively. Thus, the unique line observed in the spectrum of clintonites must be ascribed to the Si environment with 3Al in nearest tetrahedra (chemical shift values are given in Table 2). From this fact, one can conclude that no silicon atoms are present in adjacent tetrahedra of the clintonites that have been analyzed.

This observation suggests the existence in clintonites ($x_{Si} < x_{Al}$) of an energetic preference for silicon cations to be surrounded by cations of lower charge (formation of Si−O−

TABLE 2: Positions of ^{29}Si and ^{27}Al MAS NMR Components of Clintonites[a]

	Si(3Si)	Al(1Si2Al)	Al(2Si1Al)	Al_O(6Mg)	Al_O(5Mg1Al)
Si_1Al_3	−76.2	78.2	70.0	9.9	6.4
$Si_{1.12}Al_{2.88}$	−76.5	78.7	69.5	10.0	6.1
$Si_{1.25}Al_{2.75}$	−76.1	78.9	69.7	10.1	5.8
$Si_{1.33}Al_{2.67}$	−76.4	78.4	69.5	10.1	5.8

[a] Estimated errors are less than 0.5 ppm. Al_O is octahedral aluminum.

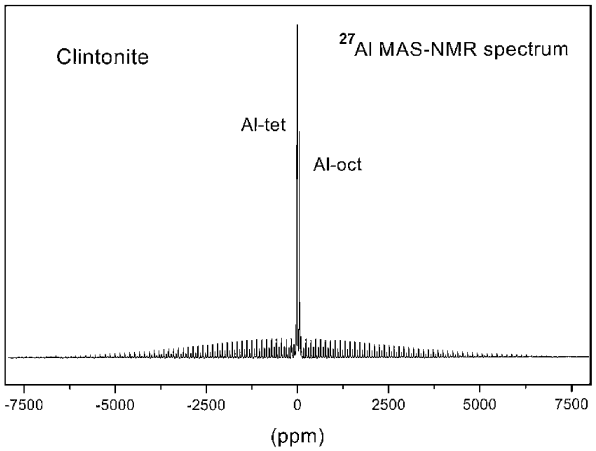

Figure 2. ^{27}Al MAS NMR spectra of a representative clintonite. Al-tet and Al-oct stand for tetrahedral and octahedral aluminum, respectively. Spectral regions covered by quadrupolar patterns result from distortions of Al polyhedra.

Al bonds). Such an observation is similar to that seen in micas in which $x_{Si} > x_{Al}$, where the same preference for the formation of Al−O−Si bonds was found with respect to Al−O−Al and Si−O−Si bridges. The main difference from the point of view of electrostatic balance is that in clintonites the minority cations (Si) have a higher charge, contrary to the case of more common micas, where minority cations (Al) have a lower charge than the most abundant (Si) cations.

Further insight into the distribution of Si and Al in clintonites can be gained from ^{27}Al NMR spectroscopy. In Figure 2, we present ^{27}Al NMR spectra of a representative clintonite, where two components at ∼75 and ∼10 ppm, associated with tetrahedral and octahedral aluminum, are detected. A spinning-sidebands pattern corresponding to satellite ($\pm^1/_2$,$\pm^3/_2$ and $\pm^3/_2$,$\pm^5/_2$) transitions of ^{27}Al NMR signals is also visible in this figure. In all cases, quadrupole C_Q and η parameters of tetra- and octahedral components were similar (3,1 MHz and 0.6), and their magnitude indicates that distortions in both polyhedra are important. A deeper analysis of the central ($-^1/_2$,$^1/_2$) transition line, corresponding to tetrahedral Al, shows the presence of two components at 70 and 78 ppm, the intensity of the first one decreasing as the tetrahedral Al content increases (see Figure 3).

In the clintonites that have been analyzed, Loewenstein's rule cannot be fulfilled, and one expects to observe several lines in ^{27}Al MAS NMR spectra, associated with different tetrahedral environments of aluminum. The two detected aluminum components are shifted toward more positive values than that detected at 63.5 ppm (3Si environment) in the phlogopite $K(Si_3Al)Mg_3O_{10}OH_2$, indicating that a larger amount of Al is present in the tetrahedra surrounding a given tetrahedron occupied by aluminum. On the basis of the chemical composition of our samples, we have ascribed the two observed components at 70 and 78 ppm to tetrahedral Al in Al(1Al2Si) and Al(2Al1Si) environments. According to this assignment, experimental results support the presence of Al−O−Al bonds, violating Loewenstein's rule (Al surrounded by 3Si) in the tetrahedral sheets of clintonite micas. In these compounds, the accumulation of negative tetrahedral charge in oxygens of Al−O−Al bridges, as compared with phlogopite, is compensated by substitution of K^+ with Ca^{2+} cations, which results in an increase in the interlayer charge in clintonites.

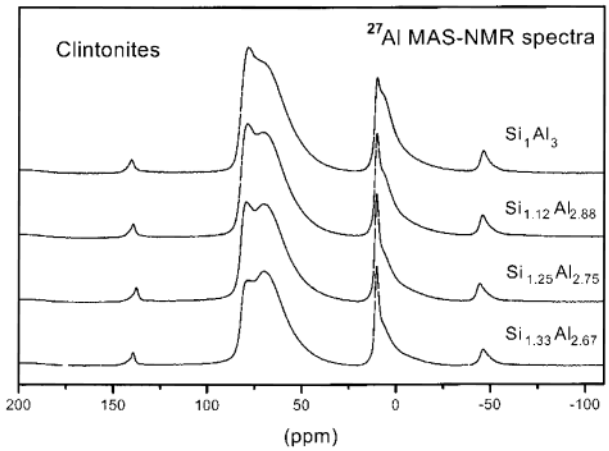

Figure 3. ^{27}Al MAS NMR spectra of clintonites with tetrahedral compositions of Si_1Al_3, $Si_{1.12}Al_{2.88}$, $Si_{1.25}Al_{2.75}$, and $Si_{1.33}Al_{2.67}$. In these spectra, the two preponderant tetrahedral components correspond to 1Si2Al and 2Si1Al environments. Narrow components near 10 ppm have been ascribed to octahedral Al surrounded by 6Mg and 5Mg1Al.

On the other hand, the presence of two environments for octahedral aluminum indicates that Al and Mg are not distributed in an ordered way in octahedral layers (occupation of M_1 sites by Al^{3+} and M_2 sites by Mg^{2+} cations). On the basis of this fact, components at 10 and 6 ppm have been ascribed to Al surrounded by 6Mg and 5Mg1Al, respectively. This assignment is compatible with the observed decrease in intensity of the 6 ppm band when Al content decreases. Positions of maxima detected in ^{27}Al MAS NMR spectra are given in Table 2.

From the spectroscopic study of clintonites, it can be concluded that silicon is surrounded by 3Al and aluminum is surrounded by different Si_nAl_{3-n} environments. However, a quantitative determination of the relative amount of different species is difficult due to line shape asymmetries caused by quadrupolar interactions in ^{27}Al NMR signals. To better analyze ^{27}Al MAS NMR spectra, two-dimensional multiquantum MQZQF experiments were carried out in samples with $x_{Si} = 0.31$ and 0.33, and the results are shown in Figure 4. One observes that isotropic spectra, corresponding to elimination of second-order quadrupolar effects, are considerably simplified (F_1 dimension). The analysis of the bidimensional plots shows that all tetrahedral Al signals display an asymmetric shape and chemical shift values near 80 ppm (intersection of lines with a slope of 10/17 with that corresponding to isotropic chemical shift values). From this fact, shoulders detected in single-pulse NMR experiments (F_2 dimension) must be ascribed to differences on second-order quadrupolar interactions at different sites occupied by aluminum. Isotropic ^{27}Al MAS NMR profiles suggest the presence of three components (1Al2Si, 2Al1Si, and 3Al environments) whose intensities change according to the sample composition. However, in all clintonites, intensities of 1Al2Si and 2Al1Si components are clearly higher than the two others.

By means of Monte Carlo simulations, one can obtain relative amounts of different environments of aluminum for different models of cation distribution in the tetrahedral sheet of phyllosilicates, and compare them with those derived from ^{27}Al

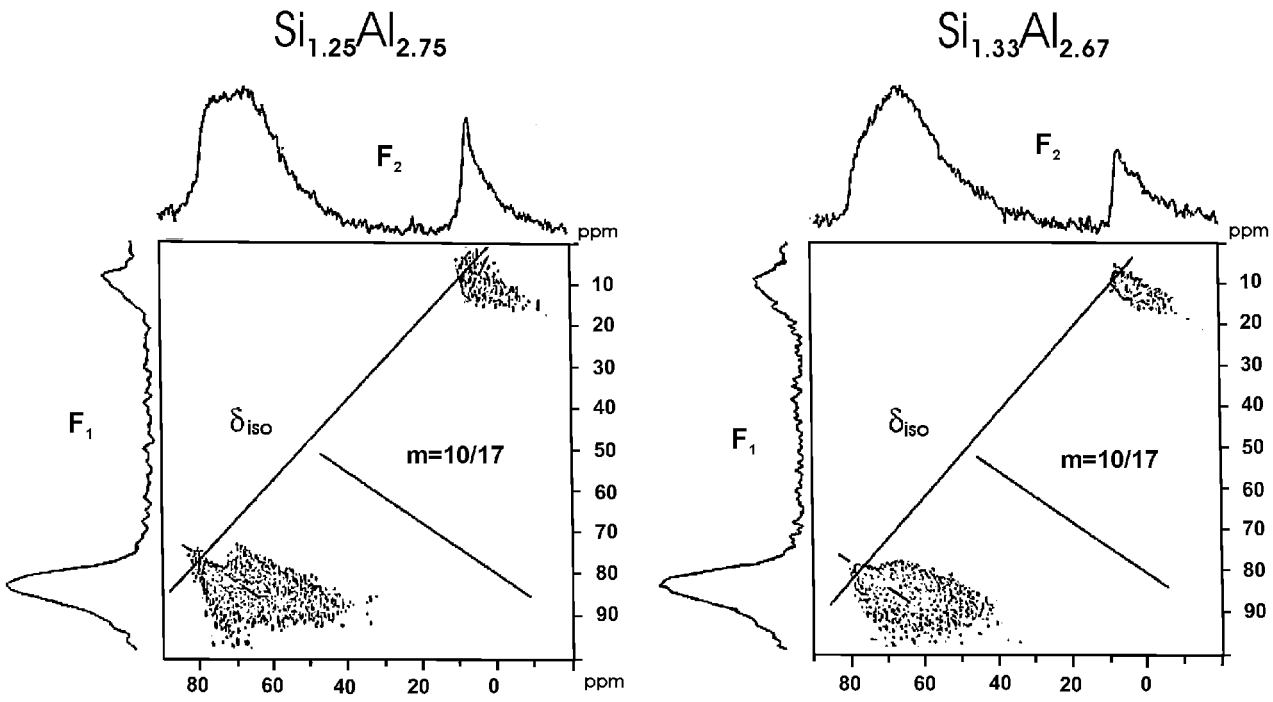

Figure 4. Two-dimensional ^{27}Al MAS NMR plots deduced from MQZQF experiments in clintonites with tetrahedral $Si_{1.33}Al_{2.67}$ and $Si_{1.25}Al_{2.75}$ compositions. On the vertical axes (F_1 dimension), second-order quadrupolar effects are minimized. Chemical shifts were estimated from the intersection of two plotted lines (see the text).

or ^{29}Si NMR spectra.[11,25] In the case of clintonites, and taking into account the absence of Si atoms in nearest tetrahedra shown above, we have first simulated cation distributions in which the avoidance of pairs of silicon cations in nearest tetrahedra was the only restriction. This means that effective interactions beyond nearest-neighbor cations are not considered ($E_2 = 0$). In Figure 5a, we present the calculated dependence of ^{27}Al NMR line intensities (normalized to 100) as a function of the Si fractional content x_{Si}, for such a model. In particular, for the ideal clintonite composition ($x_{Si} = 0.25$), this model predicts that the most intense line in the NMR spectrum should be that corresponding to the Al(1Si2Al) environment, but the Al(3Al) and Al(1Al2Si) environments should display a considerable intensity. This agrees roughly with the ^{27}Al NMR spectrum of the $x_{Si} = 0.25$ sample, where the line at 78 ppm (1Si2Al environment) is the most important component. For this clintonite, a considerable amount of hexagonal rings with 3Al and 6Al is obtained in the simulated cation distributions, besides the more abundant 4Al and 5Al ones (Figure 6a). According to these Monte Carlo simulations, the intensities of 1Al2Si and 2Al1Si bands in samples with compositions where $x_{Si} \sim 0.33$ should be close to 35%. In all spectra, intensities of 3Al and 3Si components are considerably lower than those derived from the model, indicating that apart from the avoidance of silicon cations in adjacent tetrahedra, other restrictions for the occupancy of neighboring tetrahedra must be operative in these materials.

To better analyze the influence of an additional dispersion of Si in the cation distribution, we have performed MC simulations with an E_2 of $1.3k_BT$, which coincides with the intereaction energy employed in earlier simulations of Si-rich phyllosilicates.[12] When the temperature of formation of our samples is taken into account, E_2 amounts to 2.3 kcal/mol. In this case, expected line intensities of the ^{27}Al NMR spectra of clintonites are shown in Figure 5b. For the ideal composition ($x_{Si} = 0.25$), one notices an important increase in the intensity of the NMR line associated with the Al(1Si2Al) environment, reflecting the silicon dispersion induced by the new introduced interaction (notice the different vertical scales of panels a and b of Figure 5). This is in line with the observations produced by the ^{27}Al NMR spectrum of the sample in which $x_{Si} = 0.25$. With increasing silicon loading, the intensity of the most intense line in the spectrum decreases, and becomes, when $x_{Si} = 0.33$, the same as that corresponding to the Al(2Si1Al) environment. For the ideal composition ($x_{Si} = 0.25$), we find that the amount of hexagonal rings with 3Al and 6Al is very small and almost all six-membered rings contain 4Al or 5Al cations (see Figure 6b). This fact coincides with the earlier observation of the so-called "homogeneous dispersion of charge" in Si-rich phyllosilicates, in which it was found that the number of Al (or Si) atoms in the hexagonal rings is as close as possible to the average values given by the sample composition.[25]

Since the cation distribution studied here is basically controlled by electrostatic interactions, one could expect that the distribution of Si and Al actually found in real samples should be that minimizing the electrostatic energy of the mica. This should be accomplished by a cation distribution following a criterion of maximum dispersion of charges (Si cations). A model for such a maximum dispersion of charges over the tetrahedral sheets can be realized by minimizing the number of silicon pairs in second-nearest tetrahedra. This model can in fact be simulated by our Monte Carlo procedure by increasing the effective interaction energy E_2 until the minimum number of silicon pairs is reached. The results of these simulations are shown in Figure 5c. In this case, the calculated intensity of 2Si1Al and 3Al bands in the ^{27}Al MAS NMR spectra is close to zero when $x_{Si} = 0.25$, and that of the 2Si1Al band is again close to that of the 1Si2Al band when $x_{Si} = 0.33$. In this model, long-range ordered domains are formed as shown in Figure 6c.

From the comparison of experimental results to predictions deduced from Monte Carlo simulations, it is clear that the most adequate compositions for analyzing the factors that govern the distribution of Si and Al in clintonites are those near the ideal member, Si_1Al_3. In the case where $x_{Si} = 0.33$, intensities of

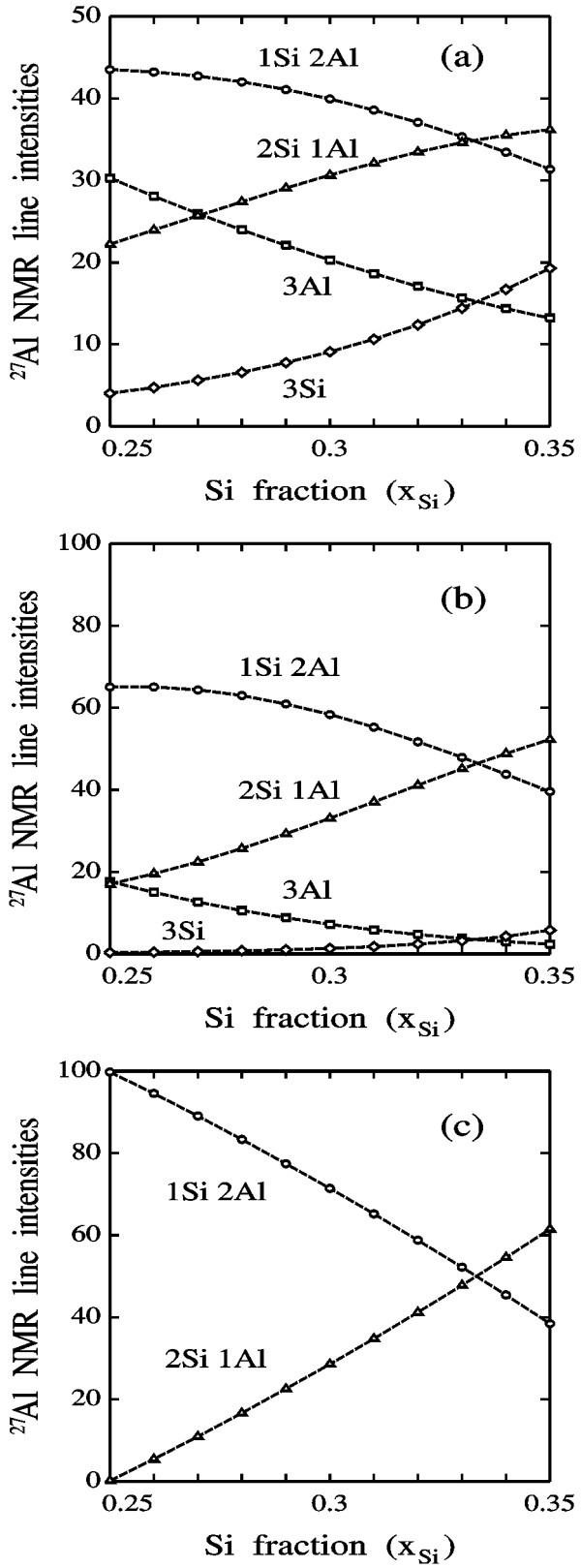

Figure 5. Calculated intensities (normalized to 100) of lines appearing in the ^{27}Al MAS NMR spectra, as a function of the Si loading in the tetrahedral sheet of clintonites. Different plots correspond to different Monte Carlo models of Si and Al distribution: (a) only Si−O−Si avoidance, (b) homogeneous dispersion of charge ($E_2 = 1.3k_BT$), and (c) maximum dispersion of charge.

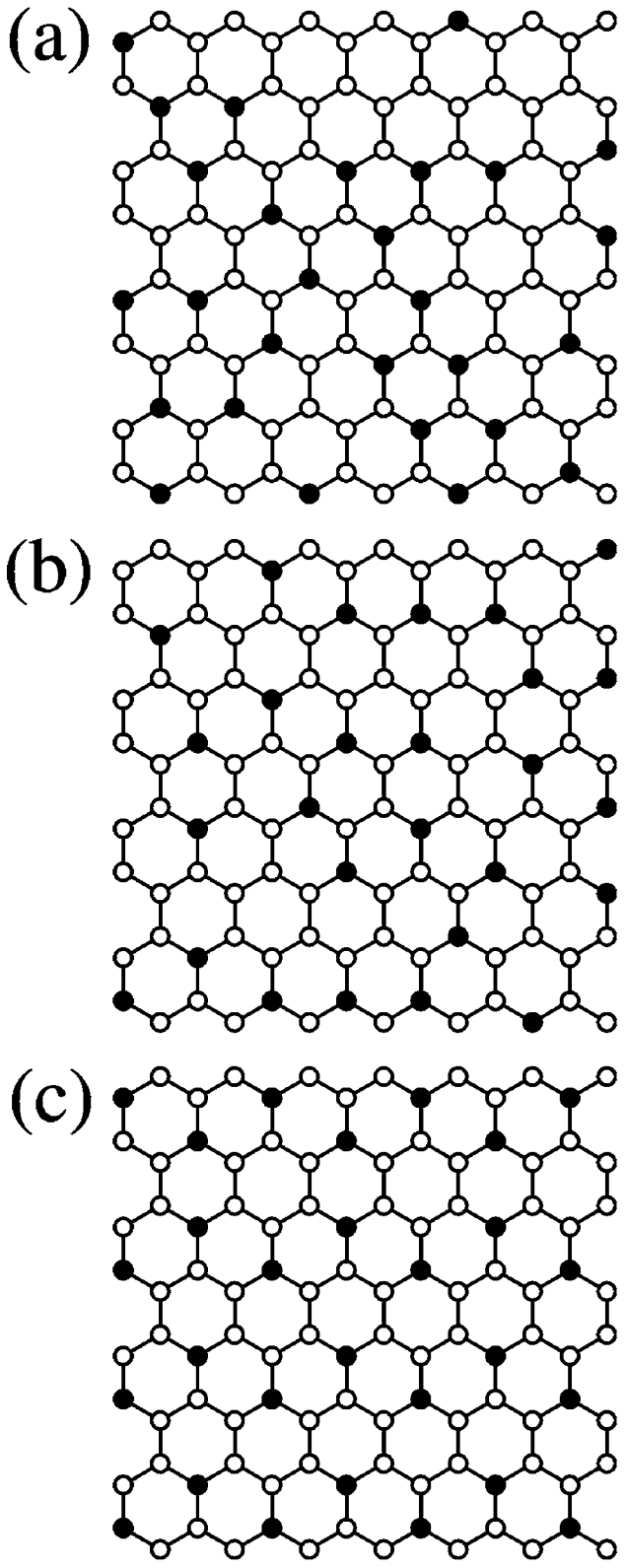

Figure 6. Tetrahedral layers of the $x_{Si} = 0.25$ composition simulated with the Monte Carlo method, taking into account the following requirements: (a) only Si−O−Si avoidance, (b) homogeneous dispersion of charge ($E_2 = 1.3k_BT$), and (c) maximum dispersion of charge. The black and white circles represent Si and Al atoms, respectively.

2Si1Al and 1Si2Al bands are nearly the same in the three models that have been considered (see panels a−c of Figure 5). From these considerations, the detection of 1Si2Al and 2Si1Al components with different intensities, along with the presence of small 3Si and 3Al components in ^{27}Al MAS NMR spectra of clintonites, indicates that the model cation distribution that best agrees with experimental results is that corresponding to a

homogeneous dispersion of charges in the tetrahedral sheets of clintonites ($E_2 = 1.3k_BT$). This kind of cation distribution is in line with that deduced earlier for samples in which $x_{Si} > x_{Al}$, in which besides the Al−O−Al avoidance[10] an additional dispersion of Al was found.[11] In the case of clintonites, in which $x_{Al} > x_{Si}$, the symmetric case is detected; besides the Si−O−Si avoidance, an additional dispersion of Si is present.

In both types of micas considered here and in earlier works, Al−O−Si groups are favored over Si−O−Si and Al−O−Al groups, what favors the dilution of Si and Al over the tetrahedral sheets. The deduced cation distribution reduces the electrostatic energy of phyllosilicates and reflects the energetic preference of cations with different charges to be diluted in the tetrahedral sheets of these minerals. This conclusion is similar to that obtained by Cohen and Burnham[26] for Na−Ca versus Na−Na and Ca−Ca pairs in pyroxenes from a minimization of the electrostatic energy. In our case, dispersion of less abundant cations can be considered an extension of Loewenstein's rule, which only takes into account the electrostratic charge balance at tetrahedral T−O−T bridges. However, the dispersion of Si cations is not maximal in tetrahedral sheets of phyllosilicates. This fact suggests that interactions between contiguous layers could also affect the tetrahedral cation distribution. The homogeneous dispersion of the tetrahedral charge favors the simultaneous disposition of hexagonal rings with 2Si4Al and 1Si5Al around interlamellar (Ca^{2+}) cations in clintonites. The presence of these two kinds of tetrahedral rings around Ca^{2+} cations ensures an efficient local balance of interlamellar charge. Finally, the results described here suggest that both enthalpy and entropy factors are significant contributions to the free energy of these minerals. At the temperatures used during their preparation, an equilibrium between the electrostatic energy (which favors the silicon dispersion) and the entropic term (which favors a disordered cation distribution) is obtained.

Conclusions

The combination of NMR spectroscopy with Monte Carlo simulations has permitted elucidation of the main characteristics of the short-range atomic order in the tetrahedral sheets of clintonites (phyllosilicates in which $x_{Al} > x_{Si}$). In these aluminum-rich phyllosilicates, a silicon−silicon avoidance in adjacent tetrahedra has been detected, similar to the well-known Loewenstein's rule (Al−O−Al avoidance) in silicon-rich compounds. From the simulations carried out in this work, interactions between second-neighbor cations are found to be significant. Dilution of cations with different charge favors a homogeneous dispersion of charges, which allows a better compensation of interlayer cationic charges. In the clintonite samples that have been analyzed, no indications of long-range ordered distributions of Si and Al have been found.

Acknowledgment. We thank Dr. L. Delevoye (Bruker-Franzen Analytik GmbH, Bremen, Germany) for the results of ^{27}Al MQZQF-MAS experiments carried out on clintonites.

References and Notes

(1) Guggenheim, S. In *Micas*; Bailey, S. W., Ed.; Reviews in Mineralogy; Mineralogical Society of America, 1984; Vol. 13, p 61.
(2) Joswig, W.; Amthauer, G.; Takéuchi, Y. *Am. Mineral.* **1986**, *71*, 1194.
(3) MacKinney, J. A.; Mora, C. I.; Bailey, S. W. *Am. Mineral.* **1988**, *73*, 365.
(4) Alietti, E.; Brigatti, M. F.; Poppi, L. *Am. Mineral.* **1997**, *82*, 936.
(5) Klinowski, J.; Thomas, J. M.; Fyfe, C. A.; Gobbi, G. C. *Nature* **1982**, *296*, 533.
(6) Lipmaa, E.; Samoson, A.; Magi, M. *J. Am. Chem. Soc.* **1986**, *108*, 1730.
(7) Engelhardt, G.; Michel, D. *High-resolution solid state NMR of silicates and zeolites*; Wiley: New York, 1987.
(8) Putnis, A.; Angel, R. J. *Phys. Chem. Miner.* **1985**, *12*, 217.
(9) Klinowski, J.; Carr, S. W.; Tarling, S. E.; Barnes, P. *Nature* **1987**, *330*, 56.
(10) Loewenstein, W. *Am. Mineral.* **1954**, *39*, 92.
(11) Herrero, C. P.; Sanz, J.; Serratosa, J. M. *J. Phys. Chem.* **1989**, *93*, 4311.
(12) Herrero, C. P.; Sanz, J. *J. Phys. Chem. Solids* **1991**, *52*, 1129.
(13) Palin, E. J.; Dove, M. T.; Redfern, S. A. T.; Bosenick, A.; Sainz-Diaz, C. I.; Warren, M. C. *Phys. Chem. Miner.* **2001**, *28*, 534.
(14) Herrero, C. P. *J. Phys. Chem.* **1991**, *95*, 3282.
(15) Gordillo, M. C.; Herrero, C. P. *Chem. Phys.* **1996**, *211*, 81.
(16) Gordillo, M. C.; Herrero, C. P. *J. Phys. Chem.* **1996**, *100*, 9098.
(17) Dove, M. T.; Heine, V. *Am. Mineral.* **1996**, *81*, 39.
(18) Vinograd, V. L.; Putnis, A. *Phys. Chem. Miner.* **1998**, *26*, 135.
(19) Hamilton, D. L.; Henderson, C. M. B. *Mineral. Mag.* **1968**, *35*, 832.
(20) Roux, J.; Vofinger, M. *J. Phys. IV* **1996**, *6*, 127.
(21) Massiot, D. *WINFIT*; Bruker-Franzen Analytik GmbH: Bremen, Germany, 1993.
(22) Massiot, D.; Touzo, B.; Trumeau, D.; Coutures, J. P.; Virlet, J.; Florian, P.; Grandinetti, P. J. *Solid State NMR* **1996**, *6*, 73.
(23) Grandinetti, P. J. *NMR*; Department of Chemistry, The Ohio State University: Columbus, OH, 1991.
(24) Binder, K.; Heermann, D. W. *Monte Carlo Simulation in Statistical Physics*, 2nd ed.; Springer: Berlin 1992.
(25) Herrero, C. P.; Gregorkiewitz, M.; Sanz, J.; Serratosa, J. M. *Phys. Chem. Miner.* **1987**, *15*, 84.
(26) Cohen, R. E.; Burnham, C. W. *Am. Miner.* **1985**, *70*, 559.